Photoconductivity in thin films of Sb_xSe_{100-x} glasses

A. S. MAAN*, D. R. GOYAL
Department of Physics, Maharshi Dayanand University, Rohtak-124 001 (Haryana) India

Photoconductivity measurements have been made as a function of temperature and intensity on thin films of Sb_xSe_{100-x} (x = 5, 10, 15 and 20) glassy alloys using a Helium Neon Laser. Temperature dependence of steady state photocurrent shows that the photoconductivity is an activated process. The activation energy of photoconduction (ΔE_{ph}) decreases with increasing antimony content. Intensity dependence of photocurrent confirms the power law dependence of photocurrent on incident radiation. Intensity exponent close to 0.5 indicates bimolecular recombination in all the alloys. Transient photoconductivity measurements have been made as a function of temperature and intensity. The decay of photocurrent comprises of two components, a faster part at the onset followed by a slower decay. Both parts of decay are found to be exponential with two distinct recombination time constants indicative of distinct processes taking part in the recombination process.

(Received August 7, 2007; accepted August 28, 2007)

Keywords: Chalcogenide glasses, Thin films, Photoconductivity, Recombination kinetics

1. Introduction

Chalcogenide glasses have received a special attention due to their wide range of applications in various solid-state devices such as switching and memory, image converters and optical mass memories etc. The presence of localized states in the mobility gap due to absence of long-range order as well as various inherent defects are common features of these glasses. The density of localized states in the mobility gap controls many physical properties of amorphous semiconductors.

Among chalcogenide glasses, amorphous Se has wide range of applications in electronics and optoelectronics. However, certain shortcomings of pure glassy Se such as short lifetime, low sensitivity and thermal instability limit its practical applications. These difficulties could be overcome by use of certain additives and especially use of Se-Sb, Se-Te and Se-Ge is of interest due to various properties like greater hardness, higher photoconductivity, and smaller ageing effects as compared to pure glassy Se. Various properties such as electrical, optical, thermal, and dielectric have already been reported in Sb-Se system by many workers [1-7].

Photoconductivity serves as a useful technique to determine the energy distribution of various kinds of gap states, which influence the carrier mobilities and lifetimes in chalcogenide glasses as attributed to multi trapping processes. These measurements are quite important to decide about the use of a particular material for various photoconductive applications. The decay of photocurrent after cessation of illumination has been reported to be non exponential [8] in some cases whereas a power law has been reported for a number of semiconducting glasses [9].

The present paper reports the photoconductivity measurements on a-Sb_xSe_{100-x} (x = 5, 10, 15 and 20 at.%) glassy alloys. The study comprises the investigation of steady state and transient photoconductivity as a function of temperature and intensity using a He-Ne laser.

The experimental details of sample preparation and photoconductivity measurements are described in section 2. Various results pertaining to steady state and transient photocurrent are presented and discussed in section 3. The last section contains the conclusions drawn from the present work.

2. Experimental

Different compositions of Sb_xSe_{100-x} glassy system (x = 5, 10, 15 and 20) were prepared in bulk form by melt quenching technique. Materials of 99.999% purity weighed according to their atomic percentage are sealed in evacuated quartz ampoules (~10^{-5} Torr). The sealed ampoules were heated to 1000^o C in an electric furnace at the heating rate of 2-3 ^{o}C /min. The ampoules were frequently rocked for about 10 hours at the highest temperature to make the melt homogenous. The quenching is done in ice-cooled water. Bulk as obtained was used for preparation of planar thin film samples by vacuum evaporation technique keeping the substrates at room temperature and base pressure of ~2×10^{-5} Torr. Indium electrodes onto a well-degassed corning glass slide were deposited by vacuum evaporation prior to deposition of sample under investigation. A planar geometry of film (length ~ 1.8 cm; electrode gap ~ 0.06 cm) was used for electrical measurements. The thickness of each film was monitored on digital thin film thickness monitor using a quartz crystal and was kept at ~ 0.5 μm for various compositions. The thin film sample was annealed in absence of light for two hours under vacuum at a fixed temperature (360 K). The photoconductivity of the amorphous films has been studied under a vacuum of 10^{-3} Torr by mounting them in a specially designed metallic sample holder having a transparent quartz window.

A Helium-Neon laser (Aerotech LSR 5P) with 25 mW maximum power was used to irradiate the sample. Intensity variation of the incident light was obtained by using glass slides and relative intensity was calculated by

calibrating with an energy meter. Using the values of energy at various illumination levels, the value of photon flux was obtained for a particular intensity. The current measurements were made using a 617 Keithley programmable electrometer with memory and data storage facility. The photocurrent (I_{ph}) is obtained after subtracting the dark current (I_d) from the current measured in the presence of light. For measurement of transient photocurrent, an optical pulse of three seconds duration of white light was used to excite the thin film samples. The rise and decay of photocurrent was stored in the programmable electrometer at a sampling rate of three data points per second. A d.c. bias of 10 volts applied by using a stabilized d.c. power supply. The temperature was measured with an accuracy of 0.1 ^oC using a $3^{1/2}$digit temperature indicator.

3. Results and discussion

Steady state photoconductivity has been investigated in thin films of Sb_xSe_{100-x} glassy alloys as a function of temperature and intensity. Fig. 1 depicts the variation of steady state photocurrent with temperature in x = 15 sample at a number of fixed intensity levels of incident radiations. The variation of dark current (I_d) with temperature is also included in the figure. As shown in the figure, $\ln I_{ph}$ vs. 1000/T plots are straight lines in the observed temperature range. Plots given in Fig. 1 suggest that the photoconductivity is an activated process with single activation energy (ΔE_{ph}) and that the activation energy for photoconduction is almost the same for different levels of illumination. Similar behavior was observed in other compositions as well. Values of ΔE_{ph} corresponding to the highest intensity level for different x values are given in Table 1 indicate that it decreases with increasing Sb content. A similar variation in activation energy of dark conduction has been observed in Sb–Se alloys [10]. It can be seen from Table 1, that $I_{ph} > I_d$ at room temperature, whereas, the parameter I_{ph}/I_d decreases with increasing temperature and finally I_{ph} becomes less than I_d.

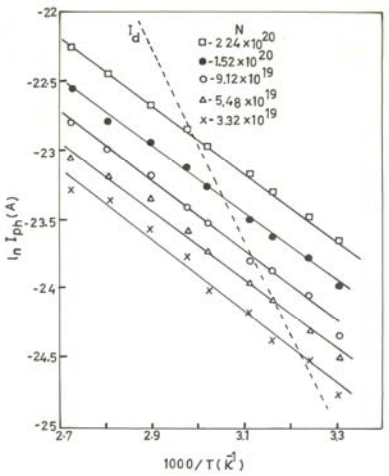

Fig. 1. Variation of steady state photocurrent with temperature at a number of fixed intensity levels in $Sb_{15}Se_{85}$ thin film.

The variation of photocurrent (I_{ph}) with temperature has been predicted to comprise of three regions with different recombination kinetics and is expected to pass through a maximum [11]. The three regions are; (a) At high temperature, the photocurrent is much smaller than dark current (I_d) and decreases with increasing temperature, (b) an intermediate region, where photocurrent increases with temperature and passes through a maximum while entering high temperature region, (c) at low temperatures the density of photocarriers is much higher than the dark carriers and does not fall as rapidly as in region (b) and tends to attain a constant value. The maxima in temperature dependence occur near the temperature where the density of dark carriers equals to those of the photo-generated carriers [12]. However, maximum in photocurrent with temperature could not be observed in present system in the observed temperature range though there has been a crossover in I_d and I_{ph} curves. A similar behavior of photocurrent with temperature has been reported in number of alloys [13,14].

To further probe into the nature of recombination mechanism, steady state photoconductivity measurements have been made as a function of incident intensity at a number of fixed temperatures. Fig. 2 shows the intensity dependence of photocurrent in thin films of x = 15 alloy. A similar behavior is observed in other compositions as well. As shown in the figure, photocurrent increases with intensity and obeys the power law $I_{ph} \alpha F^{\gamma}$. Using the slope of the curves in Fig. 2, values of the intensity exponent (γ) at different temperatures are calculated and are inserted in the figure.

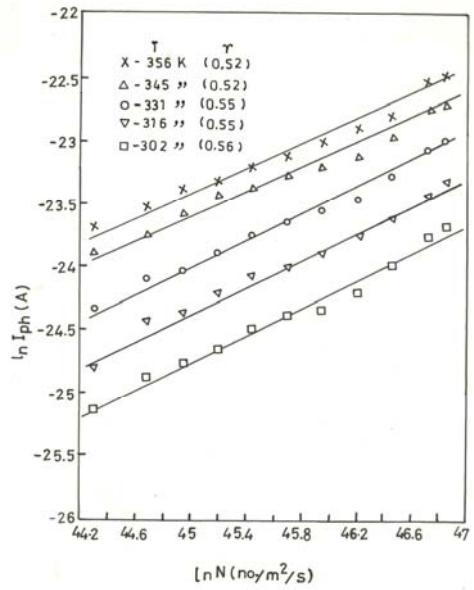

Fig. 2. Variation of steady state photocurrent with intensity at a number of fixed temperatures in $Sb_{15}Se_{85}$ thin film.

The subject of trapping and the effect of traps is quite important for discussion of photoconductivity as trapping is the fundamental process for energy storage in all electronically active solids [15]. The energy storage is

accomplished by the spatial localization of an excited electron or hole, in such a way that the charge carrier is prohibited from moving freely unless supplied with optical or thermal energy. In case of semiconductor with only one type of recombination center, the excess electron density (Δn) can be related to the generation rate G as [16]

$$G = C_n (\Delta n^2 + 2n_0 \Delta n) \quad (1)$$

C_n being the capture coefficient and n_0 is the density of thermal carriers. The monomolecular recombination is expected to take place [16] when excess carrier density is much smaller than thermally generated carrier density i.e. $\Delta n << n_0$, equation (1) reduces to

$$\Delta n = \frac{G}{2 C_0 n_0} \quad (2)$$

As generation rate is proportional to the light intensity (F), the photocurrent will vary linearly with light intensity (γ = 1.0). However, if excess carrier density is much greater than thermally generated carrier density ($\Delta n >> n_0$), equation (2) reduces to

$$\Delta_n = \left(\frac{G}{C_n} \right)^{1/2} \quad (3)$$

indicating that photoconductivity will be proportional to square root of light intensity resulting in bimolecular recombination. (γ = 0.5).

In present set of glasses, $I_{ph} > I_d$ at room temperature and γ values close to 0.5 are in confirmation with the mechanism of bimolecular recombination. For comparison sake, γ values for different compositions at room temperature (302K) are given in Table 1. For a given material, the photosensitivity (I_{ph} /I_d) is an important parameter to decide its use in photoconductive applications. I_{ph}/I_d values for different compositions have been calculated at the highest intensity at room temperature and are inserted in Table 1. One can clearly see that photosensitivity increases with increasing Sb %. Similar behavior is present at other temperatures as well.

Table 1. Various photoconductivity parameters for different compositions of Sb_xSe_{100-x} glassy system.

x	ΔE_{ph} (eV)	I_{ph}/I_d at 302 K	γ at 302 K	τ_{eff} (s) at 325 K
5	0.29	1.88	0.48	0.50
10	0.26	1.26	0.57	0.45
15	0.22	6.02	0.56	0.40
20	0.20	8.68	0.51	0.21

With a view to supplement the steady state measurements, transient photoconductivity studies have also been carried out in thin films of Sb_xSe_{100-x} glassy alloys. For each of the four compositions, transient measurements comprise of two parts (i) as a function of intensity at a fixed temperature (ii) as a function of temperature at the highest level of incident radiation. Fig. 3 shows the rise and decay of photocurrent with time in x =15 composition at different intensity levels of incident radiation.

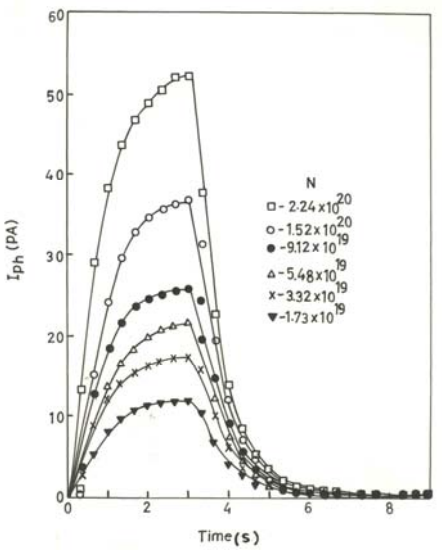

Fig. 3. Rise and decay of photocurrent (I_{ph}) with time (t) at various intensities at a fixed temperature (302 K) in $Sb_{15}Se_{85}$ thin film.

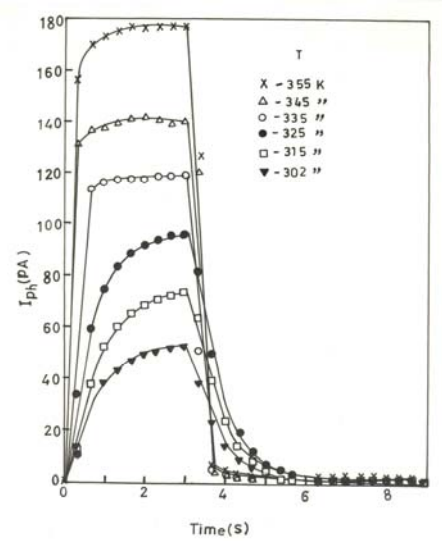

Fig. 4. Rise and decay of photocurrent (I_{ph}) with time (t) at different temperatures at highest intensity level (2.24×10^{20} photons/m^2/s) in $Sb_{15}Se_{85}$ thin film.

The variation of transient photocurrent with time at a number of temperatures is shown in figure 4 for x = 15 alloy at a fixed photon flux of 2.24×10^{20} (photons/m^2/s). As seen from various plots in both the figures 3 and 4, that the rise and decay of photocurrent with time is quite slow. Results of similar nature were obtained in other compositions. The decay process seems to be composed of two processes, a faster decay at the onset of transient and a slower decay later on. A persistent photocurrent (the asymptotic value of the current in the decay curve) is observed in all samples at different temperatures, which

does not decay even after a long time interval. This persistent photocurrent, which does not simply seems to be due to carriers trapped in the deep localized states [17] has been subtracted from the observed photocurrent. This corrected photocurrent is used for further analysis.

The decay of photocurrent strongly depends upon the characteristics of traps in a given material. When subjected to exciting radiations, certain proportion of generated free carriers is captured by traps. The traps filled during excitation will be emptied after the cessation of illumination depending upon their capture cross-section and energy depth. If the retrapping of carriers freed from traps is negligible then an exponential decay of photocurrent is expected provided the traps are monoenergetic [15] and is guided as

$$I_{ph}(t) = I_o\exp(-t/\tau) \quad (4)$$

where $I_{ph}(t)$ is the value of the current at time t after the cessation of illumination and I_o corresponds to the photocurrent at t = 0. τ denotes the decay time constant and does not change with time unlike differential lifetime in dispersive transport [18]. However if there are traps of different kinds, then the resulting decay will be a sum of many exponential terms [15], each corresponding to a different set of traps and the plots of $\ln I_{ph}$ versus time will be a combination of different slopes.

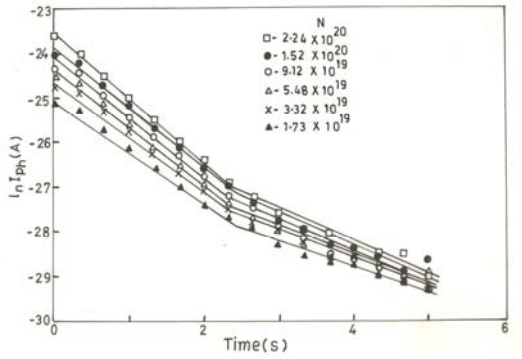

Fig. 5. Decay of photocurrent ($lnI_{ph,}$ corrected) with time (t) at different intensities at a fixed temperature in $Sb_{15}Se_{85}$ thin film (values obtained from Fig. 3).

To analyze the experimental results the decay of photocurrent at different intensity levels of figure 3 is re-plotted in Fig. 5 on a semi-logarithmic scale with time. In present set of glasses, the decay of photocurrent is exponential and consists of two distinct parts, a fast component in the beginning and a slower decay afterwards, with different values of the decay time constants. In line with the discussions as before, the decay seems to follow the relation

$$I_{ph}(t) = I_1\exp(-t/\tau_1) + I_2\exp(-t/\tau_2) \quad (5)$$

Where I_1 and I_2 are the pre-exponential factors and τ_1 and τ_2 are the decay time constants for fast and slow parts respectively. The values of decay time constants τ_1 and τ_2 for both the portions can be calculated from the experimental results.

Table 2. Decay time constants for $Sb_{15}Se_{85}$glassy alloy at different intensity levels at room temperature.

Intensity ($n_o./m^2/s$)	τ_1 (s)	τ_2 (s)	$\tau_{eff.}$ (s)
2.24×10^{20}	0.76	1.23	0.47
1.52×10^{20}	0.79	1.36	0.50
9.12×10^{19}	0.79	1.46	0.51
5.48×10^{19}	0.82	1.58	0.54
3.32×10^{19}	0.86	1.81	0.58
1.73×10^{19}	0.93	1.90	0.62

As seen in Fig. 5 for x = 15 alloy, the decay of photocurrent is exponential and consists of two different parts; as represented by equation (5), a faster part at the onset of decay process followed by a slower decay. These two processes are present at all intensities and the corresponding decay time constants τ_1 and τ_2 for faster and slower components have been calculated from the slopes of the decay curves and are inserted in Table 2. Decay of a similar nature has been reported in number of alloys where two type of traps lead to twin exponential decay [19,20]. Shallow traps gave rise to fast component and deep traps were said to be responsible for the slower part of the decay.

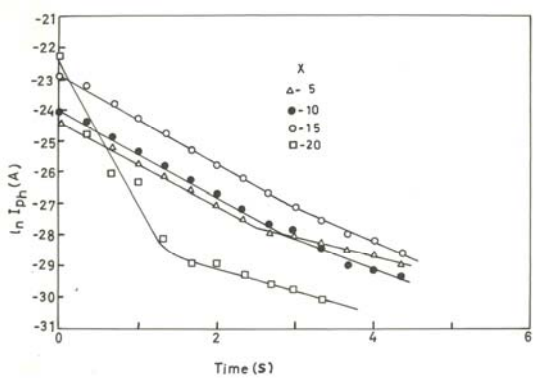

Fig. 6. Decay of photocurrent ($lnI_{ph,}$ corrected) with time (t) in Sb_xSe_{100-x} thin films at highest intensity level (2.24×10^{20} photons/m^2/s) at a fixed temperature (325 K).

For the sake of comparison, figure 6 shows the decay of photocurrent with time in different compositions at a fixed temperature (325K) and at maximum intensity level. The resulting decay is similar in nature in all four compositions and values of τ_1 and τ_2 have been obtained for each alloy. In order to have a rational comparison of the decay time constants, the concept of effective decay constant is introduced. In case of two processes with different decay time constants τ_1 and τ_2 participating in a mechanism simultaneously, then the effective time constant [21] is given as

$$1/\tau_{eff.} = 1/\tau_1 + 1/\tau_2 \quad (6)$$

The values of decay time constants for various compositions have been calculated and are listed in Table 1. τ_{eff} values indicate that the decay of photocurrent gets faster with increasing Sb%, which indicates reduction in the density of localized states in the mobility gap of Sb-Se alloys.

To analyze the effect of temperature on decay process, data of Fig. 4 is replotted on a semi-logarithmic scale as shown in Fig. 7. As seen from Fig. 7, the decay of photocurrent is twin exponential at various temperatures in x = 15 alloy. Values of τ_1, τ_2 and $\tau_{eff.}$ have been calculated using various plots in Fig. 7. From the results presented in Fig. 7, one can clearly see that the fast part of the decay increases with increasing temperature. The decay of photocurrent after cessation of light is guided by the thermal freeing of the trapped charge carriers and is an activated process.

The probability of freeing a charge carrier from a trap depends in addition to other parameters upon the thermal energy available (kT) and the trap depth [15]. At low temperature, thermal energy available is small and thus the carriers trapped into deeper levels cannot be freed by thermal activation. However, as the temperature is raised, the thermal energy available increases and the deeper set of states also start participating in the decay kinetics.

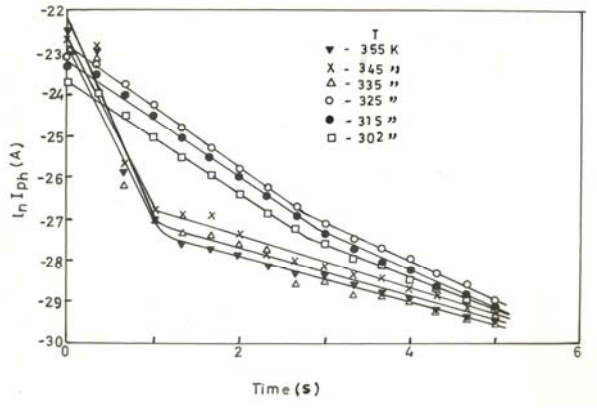

Fig. 7. Decay of photocurrent ($lnI_{ph,}$ corrected) with time (t) at different temperatures at highest intensity level ($2.24x10^{20}$ photons/m^2/sec.) in $Sb_{15}Se_{85}$ thin film (values obtained from Fig. 4).

Fig 8 depicts the variation of τ_1, τ_2 and τ_{eff} with temperature in x=15 alloy. As seen from the figure, τ_1 and τ_2 have different temperature dependence. τ_1 decreases rapidly with temperature, whereas, τ_2 has a weak temperature dependence and in contrast increases with increasing temperature.

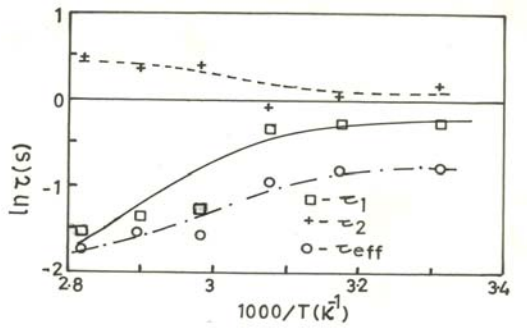

Fig. 8. Variation of decay time constants (τ_1, τ_2 and τ_{eff}) with temperature at highest intensity level in $Sb_{15}Se_{85}$ thin film.

τ_{eff} has temperature dependence similar to that of τ_1 indicates that the resulting recombination is mainly due to carriers trapped at shallow traps. A similar temperature dependence of time constants is observed in other compositions as well. Such type of temperature dependence of decay constant [22] is perhaps due to the sweeping of thermal carriers and filled recombination centers by photo-generated densities.

In a given material, I_{ph}/I_d depends upon the density of defect states. These defects may act as recombination centers in presence of light and are converted by bond switching reactions to random pairs of charged defects, known as light induced metastable defects (LIMDs) [23,24]. The charged defects act as charge trapping centers and decrease the photocurrent. A similar effect of defect states on photocurrent is reported in Se-Te-In alloys [25]. In present case, I_{ph}/I_d increases with increasing Sb% points to a reduction in the density of defect states. As seen from τ_{eff} values in Table 1, the decay becomes faster with increasing Sb content indicating a reduction in density of defect states. This behavior of τ_{eff} is in the good agreement with that of I_{ph}/I_d with composition.

4. Conclusions

The effect of variation of antimony content in Sb-Se alloys on the photoconductivity has been studied. Temperature dependence of steady state photocurrent reveals that photoconduction is an activated process and ΔE_{ph} decreases with increasing Sb%. The intensity dependence of photocurrent points to a power law dependence of photocurrent on incident radiation. $I_{ph} > I_d$ in all samples at room temperature and intensity dependence of photocurrent confirms that bimolecular recombination takes place in present set of glasses. Decay of photocurrent as a function of temperature and intensity in various compositions is exponential and consists of two parts. The concept of effective decay time constant (τ_{eff}) is used to analyze the decay of photocurrent. Temperature dependence of decay constant (τ_{eff}) shows that decay becomes faster with increasing temperature. Composition dependence of I_{ph}/I_d and τ_{eff} points to a decrease in density of localized states in the energy gap with increasing Sb content.

References

[1] V. I. Mikla, I. P. Mikhalko, V. V. Mikla, Mater. Sci. Engin. B **83, 74** (2001).

[2] M. Singh, D. R. Goyal, A. S. Maan, J. Phys. and Chem. Sol. **60,** 877 (1999).

[3] V. S. Kushwaha, D. Kumar, A. Kumar, J. Optoelectron. Adv. Mater. **8,** 1356 (2006).

[4] M. A. Majeed Khan, M. Zulfequar, S. Kumar, M. Hussain, J. Modern Opt. 50(2), 251 (2003).

[5] D. Dimitrov, D. Tzocheva, D. Kovacheva, Thin Solid Films **79,** 323 (1998).

[6] N. Choudhary, A. Kumar, Turk. J. Phys. **29,** 119 (2005).

[7] V. S. Kushwaha, S. Kumar, A. Kumar, Turk. J. Phys. **29,** 349 (2005).

[8] C. Main, D. Nesheva, J. Optoelectron. Adv. Mater. **3,** 655 (2001).

[9] A. Ganjoo, K. Shimakawa, K. Kitano, E. A. Davis, J. Non-Cryst. Solids **299,** 917 (2002).

[10] A. S. Maan, D. R. Goyal and V. Singh, Proc. 46th DAE Sol. Stat. Phys. Symp. (India), **46,** 685 (2003).

[11] N. F. Mott, E. A. Davis, Electron Processes in Non-Crystalline Materials, Clarendon Press, Oxford (1979).

[12] K. Weiser, R. Fischer and M.H. Brodsky, Proc. **10th** Intl. Semicond. Conf. Cambridge, USA, 667 (1970).

[13] A. S. Maan, A. K. Sharma, D. R. Goyal, A. Kumar, J. Non Crystalline Solids, **104,** 273 (1988).

[14] R. T. S. Shiah, R. H. Bube, J. Appl. Phys., **47,** 2005 (1976).

[15] R. H. Bube, Photoconductivity in Solids (John Wiley and Sons Inc, 1979).

[16] P. Nagels, Amorphous Semiconductors, ed. M. H. Brodsky, (Springer Verlag, Berlin Heidelberg 1979).

[17] M. Igalson, R. Trykozoko, Solid State Comm., **40**, 99 (1981).

[18] W. Fuhs, D. Meyer, Phys Stat Solidi (a), **24,** 275 (1974).

[19] J. R. Haynes, J. A. Hornbeck, Phys. Rev., **100** 606 (1955).

[20] A. S. Maan, D. R. Goyal, A. Kumar, J. Non Cryst. Solids, **110**, 1384 (1989).

[21] Aldert Vander Ziel, Solid State Physical Electronics, (Prentice Hall India, 1971) 119.

[22] C. Main, A. E. Owen, Electronic and Structural Properties of amorphous semiconductors (Academic Press, London and New York, 1973).

[23] K. Shimakawa, J. Non Cryst. Solids **77,** 1253 (1985).

[24] K. Shimakawa, A. V. Kolobov, S. R. Elliot, Adv Phys. **44**, 475 (1995).

[25] V. Sharma, A. Thakur, N. Goyal, G. S. S. Saini, S. K. Tripathi, J. Optoelectron. Adv. Mater. **7**, 2103 (2005).

*Corresponding author: asmaan66@rediffmail.com